IOSR Journal of Applied Chemistry (IOSR-JAC)
e-ISSN: 2278-5736.Volume 9, Issue 10 Ver. II (October. 2016), PP 48-64
www.iosrjournals.org

NMR (^{13}C, ^{17}O) and Vibration (IR/Raman) Studies of Bi-nuclear Carbonyls: A DFT Study

M. L. Sehgal[a,*], Amit Aggarwal[b,*] and Sunaina Singh[b]
[a]*Former Head, Department of Chemistry, D.A.V. College, Jalandhar-144008, Punjab, India.*
[b]*Department of Natural Sciences, LaGuardia Community College of The City University of New York, 31-10 Thomson Avenue, Long Island City, New York, 11101, USA*

Abstract: *DFT implemented in ADF 2012.01 was applied to 9 bi-nuclear transition metal carbonyls: [$M_2(CO)_{10}$], (M=Mn, Tc, Re), [$Co(CO)_4$–M–$Co(CO)_4$], (M=Zn, Cd, Hg), [$Fe_2(CO)_9$], [terminal $Co_2(CO)_8$] and [bridged $Co_2(CO)_8$] to obtain the Shielding Constants (σ M, $\sigma^{13}C$, $\sigma^{17}O$), Chemical Shifts (δ M, $\delta^{13}C$, $\delta^{17}O$), two diamagnetic and four paramagnetic contributing terms in the σ values of constituents. The software was also run with Frequencies and Raman full to obtain frequencies of the normal modes of all the (3n-6) Fundamental vibration bands of the carbonyls. Neither of two metals nor any two carbonyls (Cos) were found to be both spatially and magnetically equivalent. In eight of the nine carbonyls, the two metals were only spatially equivalent along with many CO groups. A perturbing metal and spatially equivalent responding metal along with spatially equivalent CO groups had same **k** and **j** values respectively. The importance of this study would lie in the fact that using these parameters, we successfully studied 4 characteristics: spatial displacements/ stereochemical equivalences of constituents; calculated Effective Spin Hamiltonian (H^{Spin}) of metals and ^{13}C nuclei, obtained Coordination Shifts ($\Delta_\delta{}^{13}C$, $\Delta_\delta{}^{17}O$); lent credence to IR / Raman results in supporting the π-acidity of carbonyls which were never studied by Comutational NMR methods.*

Keywords*: Chemical Shift, Shielding Tensor, Paramagnetic Tensor, Effective Spin Hamiltonian, Magnetic Equivalence*

I. Introduction

Transition metal carbonyls plays a key role in many areas of organometallic synthesis and industry because of their high reactivity. Carbon monoxide (CO) being a small molecule with a simple electronic structure simplifies the analysis from a ligand field theory perspective as higher symmetry gives more degeneracy. As a ligand, $\sigma^{13}C$ and $\delta^{13}C$ values obtained from its ^{13}C NMR spectra gives more information about the stereochemical equivalence/nonequivalence of the metals and of the various carbonyl groups that can serve as a guide for the substitution of the carbonyl groups by other ligands to form mixed carbonyl- ligand complexes.

The experimentally determined Chemical Shift values were reported earlier for some bi-nuclear carbonyls such as *fac*-$[Mn_2CO)_9(SbPh_3)]$, $[Mn(CO)_5(SbPh_3)][CF_3SO_3]$ and *fac*-$[Re(CO)_3Cl(SbPh_3)_2]$[1] binuclear manganese carbonyl cyanides[2], unsaturated binuclear butadiene iron carbonyls[3], heptacarbonyldiosmium and hexacarbonyldiosmium[4, 5]. Density functional theory (DFT) has been proven to be a resourceful computational tool for theoretical studies of a wide range of transition metal complexes[6-9] and other physicochemical process[6, 7]. DFT was used to study NMR parameters such as Chemical shifts and structural properties of binuclear carbonyls of 1st,2nd and 3rd transition series, binuclear rhodium(I) mixed carbonyl carboxylate[10], unsaturated heptacarbonyldiruthenium and hexacarbonyldiruthenium[11]. Homoleptic carbonyls of second-row transition metals were studied by Hartree–Fock (H-F) and DFT methods[12].

Schreckenbach et al. used DFT method to study ^{13}C and ^{17}O NMR spectra of some mono-nuclear transition metal carbonyls to obtain their chemical shifts (δ), total NMR shielding constant (σ) parameters and bond dissociation energies[13-15]. We and others have previously reported the DFT studies of some mono-nuclear metal carbonyls to calculate NMR parameters like Shielding Constants (σM ,$\sigma^{13}C$,$\sigma^{17}O$), Chemical Shifts (δ M, $\delta^{13}C$, $\delta^{17}O$),two diamagnetic and four paramagnetic contributing terms in the σ values of constituents, **k** and **j** values, Effective Spin Hamiltonian (H^{Spin}) of the metals and ^{13}C nuclei along with the Coordination Shifts($\Delta_\delta{}^{13}C$, $\Delta_\delta{}^{17}O$)[16-18]. Here we are presenting the DFT studies of seven bi-nuclear metal carbonyls: $[M_2(CO)_{10}]$ (M=Mn, Tc, Re), $[Co(CO)_4MCo(CO)_4]$ (M=Zn, Cd, Hg) and [terminal $Co_2(CO)_8$] having only terminal CO groups, along with two other bi-nuclear metal carbonyls $[Fe_2(CO)_9]$, and [bridged $Co_2(CO)_8$] that contain both terminal and bridged CO groups. All of these bi-nuclear metal carbonyls obey the18 electron rule with metals in the zero oxidation state.

The research work was subdivided as follows:

(a) Structures of the aforementioned nine bi-nuclear metal carbonyls with explanation of their NMR parameters,Spatial and Magnetic Equivalence of the two metals and the various CO groups.

(b) Calculation of Effective Spin Hamiltonian (H^{Spin}) of the two metals and the ^{13}C nuclei,the division of (3n-6) fundamental vibration bands into Vibration Symmetry Classes and their IR/ Raman activities.

(c) Discussion on the corroboration of the calculated NMR parameters with the reported IR and Raman results.

Need of the study

Three points necessitated this study were as:

(a) No computational NMR studies were reported on the bi-nuclear metal carbonyls to ascertain the *spatial displacements/ stereo chemical equivalences* and magnetic equivalence of two constituent metals and the various CO groups.

(b) Effective Spin Hamiltonian (H^{Spin}) an important NMR parameter used to determine the energy of NMR transitions had never been calculated by DFT for bi-nuclear metal carbonyls.

(c) DFT method had, hardly been applied to NMR parameters to ascertain the pi-acid character of bi-nuclear metal carbonyls though IR/ Raman techniques had abundantly been explored. We recently reported the use of DFT to ascertain the pi-acid character of some mono nuclear metal carbonyls[16].

II. Methodology [19, 20]

ADF (Amsterdam Density Functional) software was installed on Windows XP platform as "ADF jobs". A new directory was created using "File menu"of ADF jobs. After optimization of the studied carbonyl compounds, different commands were filled in the software to obtain IR/Raman and NMR parameters as follows:

2.1 NMR Parameters [17, 18, 21, 22]

The software was run by filling in certain commands like *Single Point, LDA, Default, None, Collinear, Nosym* using DZ or *TZP Basis sets.* The *Unrestricted* command was left blank. Then "NMR Program" was run in three steps:

1. The Shielding Constants (σ M, $\sigma^{13}C$, $\sigma^{17}O$) and the Chemical Shifts (δ M, $\delta^{13}C$, $\delta^{17}O$) of the constituents of various metal carbonyl compounds along with the values of two diamagnetic (diamagnetic core and diamagnetic valence tensor) and four paramagnetic contributributing terms (paramagnetic (b^) tensor**,** paramagnetic (u^) tensor**,** paramagnetic (s^) tensor and paramagnetic gauge tensors) were obtained. from the *"NMR Program"* by clicking on numbers of the species and *printing* them along with "*Isotropic Shielding Constants"* and "*Full Shielding Constants".*
2. **k** and **j** values of constituents were obtained from the same program by *using a new Input File* and printing numbers of *Perturbing* and *Responding nuclei*. Two more NMR parameters namely Effective Spin Hamiltonian (H^{spin}) and Coordination Shifts ($\Delta_\delta{}^{13}C$, $\Delta_\delta{}^{17}$ were calculated from the **j** values of M and ^{13}C.
3. $\sigma^{13}C$, $\sigma^{17}O$,$\delta^{13}C$, $\delta^{17}O$, **k** and **j** of ^{13}C and ^{17}O of C and O of uncoordinated CO (g) were obtained by repeating the above mentioned two steps with reference values $\sigma^{13}C$(-34.44) and $\sigma^{17}O$ (-129.53).

2.2. IR and Raman Parameters [13, 14]

After *Optimization*, the software was run with *Frequencies* and *Raman full* to obtain frequencies values of the normal modes of all the (3n-6) Fundamental vibrational bands of the carbonyls.

III. Results

Table 1 showed the various abbreviations and their expanded names used in this paper. Tables 2 and 3 showed the optimization[23] and thermal parameters of binuclear metal carbonyls studied. Table 4 showed the Shielding Constants (σ) and Chemical Shifts (δ) values of various constituents of bi-nuclear metal carbonyls. Six magnetic terms constituting two diamagnetic (represented by "**a**" and "**b**") and four paramagnetic terms (represented by "**c-f**") shown in Tables 5-7 were presented in three parameters as σ M, $\sigma^{13}C$, and $\sigma^{17}O$. The total values of these six magnetic terms shown in Table 8. Table 9 showed the Spatial Classification of the two metals and the various CO groups. Table 10 showed the ADF numbers of ^{13}C nuclei bonded to1st and 2nd metals. Table 11 showed **k**, **j** and H^{spin} values of metal atom nuclei. Table 12 showed the (3n-6) fundamental bands of carbonyls in terms of their IR and Raman activities. Table 13 showed the bond lengths and bond strengths in $[M_2(CO)_{10}]$ (where M= Mn,Tc, Re). Table 14 showed the wave numbers and the total coordination shifts in $[M_2(CO)_{10}]$ (where M= Mn,Tc, Re). Table 15 showed the wave numbers and total coordination shifts in $M[Co(CO)_4]_2$ (where M= Zn,Cd ,Hg). Table 16 showed the wave numbers and shielding constants of $[Fe_2(CO)_9]$ and [Bgd & Ter $Co_2(CO)_8$]. Figures (1-9) of the carbonyls would give ADF numbers which were mentioned in the tables in parentheses where ever required.

IV. Discussion

NMR parameters of the nine bi-nuclear metal carbonyls were discussed as follows:

4.1. Relation among NMR parameters

The relationship between the various NMR parameters calculated using the ADF software were shown below[24]:

(a) For diamagnetic complexes σM^{n+}, σ^1H, $\sigma^{13}C$ and $\sigma^{14}N$ were equal to the sum of their corresponding values of 2 diamagnetic and 4 paramagnetic terms.

---------**(1)**

(b) Shielding Constant (σ) and chemical shifts (δ) of ^{13}C were related to each other as:

$$\delta^{13}C = 181.1 - \sigma^{13}C \qquad \text{-------- (2)}$$

(c) δ M and $\delta^{17}O$ were numerically equal to σM and $\sigma^{17}O$ but with opposite signs:

$$\left\{ \begin{array}{l} \sigma M = -\delta M \\ \sigma^{17}O = -\delta^{17}O \end{array} \right\} \qquad \text{--------- (3)}$$

(d) The Coordination Shifts ($\Delta_\delta{}^{13}C$, $\Delta_\delta{}^{17}O$) and ($\sigma^{13}C$, $\sigma^{17}O$) were related to each other as:

$$\Delta_\delta{}^{13}C = \sigma^{13}C\,(MCO) - (-34.44) \qquad \text{---------- (4)}$$

$$\Delta_\delta{}^{17}O = \sigma^{17}O\,(MCO) - (-129.53) \qquad \text{---------- (5)}$$

(e) Some of the increased electron density on carbon would also be transmitted to oxygen of CO in carbonyls to make their $\sigma^{17}O$ more than that that in CO (g).

(f) Relative spatial displacements of constituent species were reaffirmed from shielding constants of constituents {σ M, $\sigma^{13}C$(M CO), $\sigma^{17}O$(MCO)} simply by the fact that the spatially equivalent species would possess the same values of Chemical Shifts (δ) and shielding constants (σ) along with the same values of their two diamagnetic and four paramagnetic terms respectively.

(g) The CO groups bonded to two metals might differ spatially and, thus should have one or more values of σM, δM as well as the contributing two diamagnetic and four paramagnetic terms. Again, $[Fe_2(CO)_9]$ and $[Co_2(CO)_{8\ Bgd}]$ possessed both the bridging and terminal CO groups. As the bridging COs did not back accept electron cloud, electron density on bridging COs would be less than terminal COs. So, the bridging and terminal CO groups would possess different values of σ, δ and the 6 contributing terms.

(h) It would be advantageous to understand the relation between Chemical Shift (δ), Coordination Shift ($\Delta\ \delta$) and the reference values. In general:

$$\delta = \sigma - \sigma_{reference}$$

For isolated carbon, $\sigma_{reference} = -181.1$ p pm.

$\sigma_{reference}$ for carbon of CO(g) and carbon of metal carbonyls should be different because the electron densities on the isolated carbon, the carbon of CO (g) and the carbon of a metal carbonyls were always different.

(i) Parameter **(j)** related to Effective Spin Hamiltonian (H^{Spin}) **[24]** as follows:

$$H^{Spin} = 6.023\,\mathbf{j}_{A\,B}.\,I_A\,.\,I_B\,10^{17}\ MHz\ mol^{-1} \qquad \text{--------- (6)}$$

(j) Two magnetically equivalent nuclei would have the same values of **σ, δ, k** and **j** with other nuclei of the molecule in addition to having same values among themselves. Coupling between symmetry equivalent and magnetically nonequivalent nuclei would affect the appearance of NMR spectrum while coupling between both the symmetry and magnetically equivalent nuclei had no effect on NMR spectra.

(k) π-acid ligand CO should donate electron density to the metal via dative σ bond (OC→M) to increase electron density on metal. But due to the strong π back donation from the filled d orbitals of metal into the energetically suitable and geometrically favorable vacant π^* molecular orbitals of CO (OC←M), the electron

density woould be reduced on the metal to cause an increase in the electron density on carbon of CO. As σ of any nucleus was directly related to electron density, any change in the σ value would serve as an indicator to the change in its electron density. So, if CO was to act as a back acceptor, $\sigma^{13}C$ of metal carbonyls should become more than $\sigma^{13}C$ of CO(g). But according to vibration spectroscopy (IR/Raman), π back donation by CO would cause a decrease in ν_{CO} in the carbonyls with respect to uncoordinated CO(g) {ν_{CO} =2143 cm^{-1}}[25].

4.2. Structures, NMR, IR and Raman Parameters of Carbonyls

4.2.1.Trends in NMR parameters of 9 binuclear carbonyls

Following trends were observed in σ M, σ ^{13}C, σ ^{17}O values and their respective six diamagnetic and paramagnetic constituting terms:

1. Both the spatially equivalent metals possessed same σ M values (Table:4).
2. Two sets of values of σ ^{13}C and σ ^{17}O in [$M_2(CO)_{10}$] (M=Mn,Tc, Re) {Figs. 1-3} indicated two types of COs; 8 being of 1st type and 2 being of the 2nd type (Table:4).
3. [$Co(CO)_4$-M-$(CO)_4$] (M=Zn, Cd, Hg) {Figs. 4- 6} possessed two types of COs; 6 being of the 1st type and 2 of the 2nd type (Table: 4).
4. [$Fe_2(CO)_9$] {Fig. 7} showed two types of COs; 6 of 1st type and 3 of 2nd type.
5. [$Co_2(CO)_{8\ Ter}$] {Fig. 8} showed two types of terminal COs; each having 4 COs.
6. [$Co_2(CO)_{8\ Bgd}$] {Fig. 9} showed 3 types of COs; 4 of 1st type; 2 of each of 2nd and 3rd type.

4.2.2. Structures and NMR parameters of [$M_2(CO)_{10}$] (M= Mn, Tc , Re)

The carbonyl compounds [$M_2(CO)_{10}$] {M=Mn, Tc, Re} {Figs:1-3} having D_{3d} symmetry with the two metals were bonded to each other by an M-M bond. Each metal, further, formed five bonds with the carbon atom of each one of the five COs. Both the metals were spatially equivalent with same value of σ M (M= Mn, Tc, Re). There were two types of COs. Eight COs (4 on each M atom) belonged to one type (T-1) having one set of values of σ ^{13}C and σ ^{17}O and the remaining two COs (one on each M atom) were of second type (T-2) with another set of σ ^{13}C and σ ^{17}O values; no matter values were different from those of the first set (Table:10). As all the ten COs were terminal, they, all, act as back acceptors of electron and thus increases the electron density on carbon and oxygen to make their σ ^{13}C and σ ^{17}O values more than their respective reference values {$\sigma^{13}C$(-34.44) and $\sigma^{17}O$(-129.53)}. The values were, indeed, higher than the reference values in the second set consisting of two COs in all these three metal carbonyls. But two different types of behaviors were noticed in the set constituting eight COs. The $\sigma^{13}C$ values were lower in Mn(0) carbonyl than $\sigma^{13}C$ reference value but higher in Tc(0) and Re(0) carbonyls (Table: 4). This was explained as follows:

The structures of $M_2(CO)_{10}$ (M=Mn, Tc, Re) were described as two octahedra sharing one corner[26-29]. The M–M bond formed by the overlap of electron clouds of the energetically highest half filled nd_{xy} orbital (n=3, 4, 5; M= Mn, Tc, Re) on each one of the two metals joining two square pyramidal $M(CO)_5$ parts were longer because of the absence of bridging. One CO on each M was coaxial with M–M bond and the other four COs on each M atom were ⊥ to it. So the vacant nd_z^2 orbital *(n=3, 4, 5)* of each one of the two M atoms should be available to form one sigma bond with each one of the two COs. The lowest filled degenerate nd_{yz}, nd_{zx} (n=3 4,5; M= Mn,Tc,Re) set of orbitals would donate back electron cloud into the vacant π* orbitals of CO to make the electron density to increase on this set of two COs and, thereby, make σ ^{13}C more than the reference σ ^{13}C.

Conversely, lesser electron cloud density would be available from these orbitals for back donation to the remaining two sets of four ⊥COs due to their unfavorable geometry. So the σ ^{13}C of this type of eight COs was also more than the reference value but only to a small extent in the case of Tc(0) and Re(0) carbonyls. So much so, in Mn(0) carbonyl, σ ^{13}C of this type of COs was less (-39.9 ppm) than the reference value (-34.44 ppm) as the weakest Mn- Mn bond played the spoiler. Owing to an increase in metal ligand bond strength (S_{M-L}) as a result of the increased radial extension of the ndz^2 orbital (n=3, 4, 5; Mn,Tc, Re), the M-M bond strength increased in the order: Mn < Tc < Re. This was also the observed order of back donation in the three metal carbonyls as given in (Table:13).

4.2.3. Structures and NMR parameters of [$Co(CO)_4$–M–$Co(CO)_4$] {M= Zn, Cd , Hg}.

The carbonyl compounds $Co(CO)_4$–M–$Co(CO)_4$ {M=Zn, Cd, Hg} {Figs: 4-6} having D_{3d} symmetry and both the Co(0) were spatially equivalent with the same value of σ Co. Each Co(0) formed four bonds with the four terminals COs. Of the 8 terminal COs, the six COs (3 on each M atom) belong to one type (T-1) with one set of σ ^{13}C and σ ^{17}O values (Table: 4). The remaining two COs (one on each M atom) of the second type (T-2) possessed another set of values of σ ^{13}C and σ ^{17}O that were different from the first set (Table:10). As all the COs were terminal, they act as back acceptors of electron to increase the electron density on C and O and make their σ ^{13}C and σ ^{17}O values more than their reference values. But, the increase was less in the second type of COs (Table: 4). This was explained as follows: The three carbonyls possessed linear Co-M-Co structure.

They were assumed to consist of one M^{2+} (M= Zn, Cd, Hg) and two Co^{-1}. The M–M interaction was facilitated by the overlap of ns valence orbitals (n=4, 5, 6; M=Zn, Cd, Hg) of M^{2+} and the $3d_z^2$ orbital of Co^{-1} along Co-M-Co z-axis[30]. As both the COs lie along Z-axis (one bonded to each Co^{-1}) whose $3d_z^2$ orbital had, already,overlapped with ns orbitals of Zn, Cd, Hg respectively,only a little of $3d_z^2$ electron cloud was available for back donation to these two COs. So, only a little increase in $\sigma\ ^{13}C$ and $\sigma\ ^{17}O$ values were observed in these two COs groups relative to the reference values: $\sigma\ ^{13}C$ (-34.44 p pm) and $\sigma^{17}O$ (-129.53 p pm) respectively.

4.2.4. Structure and NMR Parameters of $[Fe_2(CO)_9]$

The carbonyl compound $Fe_2(CO)_9$, {Diiron nonacarbonyl} consisting of two octahedra sharing a face, and the two Fe(0) atoms were stereochemically equivalent with same value of σ Fe. The nine COs groups were of two types. The 6 terminal COs belonged to the same type (T) and thus possessed same set of $\sigma\ ^{13}C$ and $\sigma\ ^{17}O$ values. The remaining three bridging (B) COs, with another set of values of $\sigma\ ^{13}C$ and $\sigma\ ^{17}O$, that were quite different from those of the first set (Table:4). The six terminal COs would act as back acceptors of the electrons to increase the electron density on carbon and oxygen to make their $\sigma\ ^{13}C$ and $\sigma\ ^{17}O$ values more than their respective reference values. The three bridging COs behaved analogous to carbonyl group to form single bond with each one of the two Fe(0) with no back accepting properties to make their $\sigma\ ^{13}C$ and $\sigma\ ^{17}O$ values less than the reference values (Table:10) respectively. This decrease overweighed the increase brought about by terminal COs. So, the Total Coordination Shift showed a negative value(-13.74 ppm)***.** (Note: ***** -13.74= [(-11.1+34.44)*6+(-85.7+34.44)*3]

Theoretical analysis at various levels had been devoted to the electronic structure of $Fe_2(CO)_9$ to answer the question of whether a direct metal-metal bond should exist[31] or not. Such a bond was required to satisfy "The18-Electron Rule" of each metal centre as any experimentalist might argue.Theoreticians, however, were inclined to deny its existence because several arguments, e.g., the negative value of the calculated Fe-Fe overlap population (OP), better support an effective Fe-Fe repulsion.However,a detailed analysis indicated that a small direct Fe-Fe attractive interaction was hidden under this relatively large repulsion {Fig:7}.

4.2.5. Structure and NMR Parameters of $[Co_2(CO)_{8\ Ter}]$

Dicobaltoctacarbonyl $[Co_2(CO)_{8\ Ter}]$, a fluxional molecule would exists as an equilibrium mixture of two forms. One form contained a Co-Co bond with each metal atom bonded to 4 terminal COs. Two Co(0) were spatially nonequivalent with different σ Co values. Since the two σ Co(0) differed only by 0.8%, many workers assumed the two Co(0) to be spatially equivalent. The 8 terminal COs were of two types; each type consisting of 4 COs (T-1, T-2) with two different sets of $\sigma\ ^{13}C$ and $\sigma\ ^{17}O$ values. But 4 CO s having same set of $\sigma\ ^{13}C$ and $\sigma\ ^{17}O$ values were not attached to same Co(0), rather, the two COs attached to each of two Co(0) atoms. So, in $[Co_2(CO)_{8\ Ter}]$ compound, each one of the Co(0) was also bonded to two types of spatially different COs; each type having 2 spatially equivalent *COs.* This was explained as follows:

Each Co(0) was penta coordinated with one position being occupied by the other Co(0) metal atom and the remaining four positions were occupied by four COs. The two possible polyhedrons for coordination number five were: trigonal bipyramid (sp^3 manifold supplemented by the prolate $3d_z^2$ orbital with two opposite major lobes) and the square pyramid (sp^3 manifold supplemented by the oblate $3d_{x^2-y^2}$ orbital with four coplanar major lobes). The possibility of a continuous transformation of a trigonal bipyramid ($sp^3d_z^2$) to a square pyramid ($sp^3d_{x^2-y^2}$) through the linear exchange of $3d_z^2$ and $3d_{x^2-y^2}$ orbitals was related to stereo chemical non-rigidity of $[Co_2(CO)_{8\ Ter}]$ by *Berry pseudo rotation process*[32-35]. Further, a square pyramid has four coplanar vertices, i.e. four basal vertices were the border vertices as they border the square hole (base of square pyramid). The half filled $3d_{x^2-y^2}$ orbital on each Co(0) overlapped to form a Co-Co bond. Each one of the remaining set of four vacant hybrid orbitals received a lone pair of electrons from each of the four COs and then back accepted the electron cloud to increase the electron density to make their $\sigma\ ^{13}C$ and $\sigma\ ^{17}O$ values more than those of reference values. One set of two COs lying on one side of the base of square pyramid on each Co(0) received back more electron cloud than the other set of two COs. So, $\sigma\ ^{13}C$ and $\sigma\ ^{17}O$ values became more in one set of four COs [two on each Co] than the other set of four COs {Fig:8}.

4.2.6. Structure and NMR parameters of $[Co_2(CO)_{8\ Bgd}]$

The other form of dicobaltoctacarbonyl $[Co_2(CO)_{8\ Bgd}]$[36] was a doubly bridged form that also showed other intermediate isomers possessed two $Co(CO)_3$ sub-units connected by one Co-Co bond and two bridging COs{Figs:9}. The equilibrium between the two forms, terminal and bridged, implied the low energy difference between the two. Unlike $[Co_2(CO)_{8\ Ter}]$, the bridged form possessed two spatially equivalent Co(0) having the same value of σ Co. The eight COs were divided into three types. The two spatially equivalent bridging COs {B} formed a distinct class with $\sigma\ ^{13}C$ and $\sigma\ ^{17}O$ values being lower than those of the reference values as they do not back accept electron cloud. The remaining 6 terminal COs formed two spatially different classes; one having two COs (one on each M; T-1) and the other has four COs {2 on each M; T-2}. Both of these classes of terminal

COs possessed higher $\sigma^{13}C$ and $\sigma^{17}O$ values than their reference values. Formation of a variety of bonds and difference in $\sigma^{13}C$ and $\sigma^{17}O$ values was explained as follows:

$[Co_2(CO)_{8\ Bgd}]$ with C_{2v} symmetry resembled nearly to $[Fe_2(CO)_9]$ with one bridging CO group missing. Each Co(0), no doubt, was hexa coordinated but all the five 3d orbital were *non degenerate* with $3d_z^2$ and $3d_{xz}$ orbitals taking part in hybridization[37]**.** The half filled $3d_{x^2-y^2}$ orbital on each Co(0) formed a Co–Co bond. The three vacant hybrid orbitals on each Co (one lying along the Co–Co axis and other two being ⊥ to it) formed three bonds with three terminal COs. The remaining two filled hybrid orbitals on each Co(0) and the two sigma lone pairs (one lying on each carbon atom of each CO) overlapped to form four sigma bonds with two bridging COs. One terminal CO that was bonded to each Co(0) lying along the Co–Co axis should, very easily, back accept electron cloud from energetically favorable and geometrically suitable filled $3d_{xy}$ and $3d_{yz}$ orbitals of each Co(0). So electron density on these two COs increased to make their $\sigma^{13}C$ and $\sigma^{17}O$ values higher. The remaining four COs; two bonded to each Co(0) being ⊥ to the Co-Co axis received back the electron cloud to a lesser extent to show only a small increase in their $\sigma^{13}C$ and $\sigma^{17}O$ values.

4.2.7. Spatial and Magnetic Equivalence of two metals and CO groups

(a) In none of these 9 binuclear metal carbonyls, the two metal atoms and any two COs were both spatially and magnetically equivalent (Tables: 9, 10); no matter many COs were only spatially equivalent.
(b) Two Co(0) were spatially nonequivalent with different σ Co values only in $[Co_2(CO)_{8\ Ter}]$. But the difference being only 0.8%,could be neglected.
(c) A specific relationship was observed among various sets of ***k*** and ***j*** values of metals and ^{13}C of these carbonyls as explained with an example of $Mn_2(CO)_{10}$

When perturbing species was the first metal and the responding species was the spatially equivalent second metal, the **k** and **j** values remained almost the same. For example Mn(1) and Mn(2) possessed the same **k**(209.004) and **j**(152.805) values respectively in $Mn_2(CO)_{10}$ (Fig:1). For COs directly attached to one metal and their spatially equivalent COs attached to the second metal, the **k** and **j** values of ^{13}C were also found to be almost same. Again, in $Mn_2(CO)_{10}$, eight carbonyls bearing numbers (3,5,7,11,13,15,19,21) were spatially equivalent. The four carbonyls (3,5,7,11) were bonded to Mn (I) and the remaining four (13, 15,19,21) attached with Mn (2). These two sets of Cos were found to have almost same values of **k** (-3.987) and **j** (-2.983). Similarly, two COs with numbers (9,17) were spatially equivalent. Carbonyl (9) bonded to Mn (I) and carbonyl (17) bonded to Mn (2). These two sets of COs were found to have the almost same values of **k** (-12.462) and **j** (-9.284) (Table:10).

4.2.8. Calculation of Effective Spin Hamiltonian (H^{Spin}) of M and ^{13}C nuclei

A direct relationship between the two NMR parameters **j** and H^{Spin} shown above as equation **6**, helped us to determine the energy of an NMR transition. The term "effective" in effective spin Hamiltonian function implied that its solutions reproduced nuclear magnetic energy levels in a molecular system without reference to electrons. In a fictitious absence of surrounding electrons, the shielding constants and indirect spin-spin coupling constants would vanish leaving the NMR spectrum to be determined by Nuclear Zeeman Term and direct dipolar coupling. The **(j)** parameter was affected by the nature of solvent and metal−ligand bond distances and usually transmitted through the bonding electrons with its magnitude falling off rapidly with the increase in number of intervening bonds. It might have positive [*if energy of A was lower when B had opposite spin as A (α β or β α)]* or negative [*if energy of A was lower when B had same spin as A (α α or β β)]* values of energy. The H^{Spin} values of the metal ions and the bonded carbon atoms, related to their **j** values were shown in Table:11.

4.2.9. Classification of (3n-6) fundamental vibrational bands into their IR and Raman activities and the Vibration Symmetry Classes

Both the IR and Raman spectra of the 9 carbonyls were studied. Each one of the (3n-6) fundamental vibration bands was represented with a Vibration Symmetry Class having a definite vibration symmetry symbol[25]. The IR bands were classified as IR-active, Raman-active and both IR and Raman-active. In addition, some bands were Raman- active but possessed negligibly small Raman intensities and so were not observed in the spectra (Table:12). Unlike their experimental determination[38-41], here Raman intensities were calculated from the polaziabilities[42-46] and, thus, were expected to have exact values. The discussion regarding IR and Raman studies were divided into the following five parts:

1. The 60 bands in each of $M_2(CO)_{10}$ {M= Mn ,Tc ,Re } were classified into symmetry symbols A_1, A_2, B_1, B_2, E_1, E_2 and E_3 having 7,1,2,6,16,12 and 16 bands respectively. Their vibration symmetry class were represented as: $(7A_1+A_2+2B_1+6B_2+8E_1+6E_2+8E_3)$ **(**Tables: 1,12; E being doubly degenerate).

2. The 51 bands in one each of $[Co(CO)_4–M–Co(CO)_4]$, {M= Zn, Cd, Hg} were classified into symmetry symbols A_{1g}, A_{2g}, A_{1u}, A_{2u}, E_{1g} and E_{1u} having 7,1,2,7,16 and 18 bands respectively. Their vibration symmetry class was represented as $(7A_{1g}+A_{2g}+2A_{1u}+7A_{2u}+8E_{1g}+9E_{1u})$ (Tables:1,12; E being doubly degenerate)**.**

3. The 54 bands in $[Fe_2(CO)_9]$ were classified into symmetry symbols AA_1, AA_2, AAA_1, AAA_2, EE_1 and EEE_3 having 7,3,2,6,20 and 16 bands respectively. Their vibration symmetry class was represented as $(7AA_1+3AA_2+2AAA_1+6AAA_2+10EE_1+8EEE_3)$ (Tables:1,12; E being doubly degenerate).
4. The 48 bands in $[Co_2(CO)_{8\ Ter.}]$ were classified into symmetry symbols A_1, A_2, B_1 and B_2 having 15,10,11 and 12 bands respectively. Their vibration symmetry class was represented as: $(15A_1+10A_2+11B_1+12\ B_2)$ (Table:12).
5. All the 48 bands of $[Co_2(CO)_{8\ Bgd.}]$ belong to only one type of symmetry element A_1 and so its vibration symmetry class was represented as $(48A_1)$ (Table:12).

4.2.10. NMR results corroborate with reported IR and Raman results

Results obtained from the NMR studies corroborated well with the previously reported wave number [ν_{CO}] values for all the nine carbonyls. Since, the carbonyls possessed stereochemically different CO groups with different δC values, it would be better to correlate their [ν_{CO}] values with their Total Coordination Shift ($\Delta\delta C_T$**)** values that were the averaged values of δC of all the carbonyl groups in any metal carbonyl. Depending upon the similarities in their symmetry point groups, the discussion was divided into the following three parts.

(a) $[M_2(CO)_{10}]$ {M= Mn ,Tc , Re}

As the Total Coordination Shift ($\Delta\ \delta\ C_T$**)** increased, the ν_{CO} (cm^{-1}) also increased[26-29] to decrease the π -back accepting capacity of the electron cloud by the metals.The NMR studies corroborated well with IR studies because like ν_{CO}, their **(**$\Delta\ \delta\ ^{13}C_T$**)** values were also found to be highest in the rhenium carbonyl and lowest in manganese carbonyl as given in (Table:14).

(b) $[Co(CO)_4–M–Co(CO)_4]$ {M=Zn, Cd, Hg}

Total Coordination shifts ($\Delta\delta^{13}C_T$)[47] of these carbonyls did not differ much; a fact well supported by their IR[48] and Raman spectra[49] as their reported $\nu_{(CO)}$ values also differed from one another only to a small extent (Table:15).

(c) $[Fe_2(CO)_9]$, [terminal- $Co_2(CO)_8$] and [bridged- $Co_2(CO)_8$]

For terminal COs, $\sigma\ ^{13}C$ and $\sigma\ ^{17}O$ values were found to be higher than their respective reference values while their $\nu_{(CO)}$ were observed to be lower than ν_{CO} of CO (g). So the results obtained from this NMR study lent support to the already reported vibration spectral (IR/Raman) studies with respect to π –back acceptor character of carbonyls (Table:16). The reference values were: $\sigma\ ^{13}C$ (-181.1 p pm); $\sigma^{17}O$ (-129.53 ppm), and ν_{CO} Terminal ($2143cm^{-1}$).

V. Conclusions

Using DFT implemented in ADF program, we were able to reaffirm the relative spatial displacements and the π -acid character of the various CO groups for nine bi-nuclear transition metal carbonyls from the NMR parameters of ^{13}C and ^{17}O nuclei ($\sigma\ ^{13}C$, $\sigma\ ^{17}O$, $\delta^{13}\ C$, $\delta^{17}O$) along with two diamagnetic and four paramagnetic constituting terms in $\sigma^{13}C$, $\sigma^{17}O$ parameters. We were also able to confirm the spatial equivalence/nonequivalence of the two metals in these bi-nuclear carbonyls. NMR studies corroborated well with the results already obtained from their IR/Raman studies. Lastly, we could identify some bands which, no doubt, were Raman active but because of their negligible Raman intensities could not be observed in the Raman spectra.

Acknowledgements

Authors gratefully acknowledge the kind and willing cooperation of Mr. Sunil Chawla [sunil@seascapelearning.com] of ADF (http://www.scm.com).They feel indebted to Mr. S.R. Heer, Chief Engineer (Retd.), North Zone, Doordarshan, New Delhi (India), for his invaluable cooperation in the installation and smooth working of the ADF software.

VI. Author Contribution

M.L.S. acquisition data, analysis and interpretation of the data, drafting the manuscript, A.A. and S.S. rearranging and critical revision of the manuscript.

Conflict of Interest

The authors declare that they do not have conflict of interest with the content of this article.

Table: 1. Acronyms and Their Expanded Forms

Acronym	Expanded Form
DFT	Density Functional Theory
ADF	Amsterdam Density Functional
ZORA	Zeroth- Order Regular Approximation
LDA	Local Density Approximation
H-F	Hartree- Fock
DZ/ TPZ	Double Zeta/ Triple Zeta
Nosym	Normalized or True
GGA	Generalized Gradient Approximation which further contains *Exchange* and *Correlation* parts
GGABP	Generalized Gradient Approximation Becke perdew
A, A1, A2, B, B1, B2, B3	Singly degenerate; Number of bands in IR is equal to the numerical figure written along with any A or B term
E,E1, E2, E3	Doubly degenerate; Number of bands in IR/Raman is equal to double the numerical figure written along with any E term
T, T1, T2, T3	Triply degenerate term; Number of bands in IR/Raman is equal to triple the figure written along with any T term

Table: 2. Optimization Parameters of Binuclear Carbonyls

Carbonyl Dipole moment(D)	Point group	Total bonding** Energy	Total Energy: X c* (LDA) k J mol^{-1}	Nucleus	I
$Mn_2(CO)_{10}$ (0.06)	D_{4d}	-16228.38	-587055.56 (-551915.54, -35140.02)	^{55}Mn	2.5
$Tc_2(CO)_{10}$ (0.00)	-do-	-22380.35	-460561.10 (-398558.60, -30715.23)	^{99}Tc	4.5
$Re_2(CO)_{10}$ (0.08)	-do-	-16957.54	-1932590.75 (-1867855.29, -64735.5)	^{187}Re	2.5
$Co(CO)_4Zn\ Co(CO)_4$ (0.02)	D_{3d}	-13189.34	-737533.42 (-699065.34, -38468.08)	^{59}Co ^{65}Zn	3.5 2.5
$Co(CO)_4Cd\ Co(CO)_4$ (0.00)	-do-	-13183.63	-942263.67 (-898793.66, -43470.01)	^{59}Co ^{112}Cd	3.5 0.5
$Co(CO)_4Hg\ Co(CO)_4$ (0.02)	-do-	-13196.23	-1452311.69 (-1398925.27, -53406.5)	^{59}Co ^{201}Hg	3.5 0.5
$Fe_2(CO)_9$ (0.06)	D_{3h}	-14804.54	-572444.87 (-539144.44, -33300.43)	^{57}Fe	0.5
$Co_2(CO)_8$ Bgd (0.00)	C_{2v}	-13028.21	-558646.56 (-527167.98,-31478.58)	^{59}Co	3.5
$Co_2(CO)_8$ Ter (0.05)	D_{3d}	-12960.31	-558646.04 (-527167.55, -31478.48)	^{59}Co	3.5

*****Xc consists of LDA and GGA components; both contain *Exchange* and *Correlation* parts**Bonding energy is computed as energy difference between molecule and fragments. GGA=0 for all these 9 binuclear transition metal carbonyls.

Table: 3. Thermal Parameters of Binuclear Carbonyls at 298 K

Carbonyl	Zero Point Energy (e V)	Some Thermal Parameters											
		Entropy (cal mol^{-1}K^{-1})				Internal Energy (Kcal mol^{-1})				Constant Volume Capacity (Kcal mol^{-1} K^{-1})			
		Trans.	Rot.	Vib.	Total	Trans.	Rot.	Vib.	Total	Trans.	Rot.	Vib.	Total
$Mn_2(CO)_{10}$	1.831	43.774	30.39	53.85	128.013	0.889	0.889	51.127	52.904	2.981	2.981	50.52	56.481
$Tc_2(CO)_{10}$	1.885	44.369	30.66	46.30	121.33	-do-	-do-	51.615	53.392	-do-	-do-	49.56	55.524
$Re_2(CO)_{10}$	1.904	45.315	30.94	44.07	120.319	-do-	-do-	51.798	53.576	-do-	-do-	49.13	55.052
$Co(CO)_4Zn$ $Co(CO)_4$	1.146	42.107	28.97	27.80	98.872	-do-	-do-	31.043	32.820	-do-	-do-	20.03	25.993
$Co(CO)_4Cd$ $Co(CO)_4$	1.439	44.239	31.66	58.57	134.790	-do-	-do-	42.788	44.555	-do-	-do-	49.87	55.831
$Co(CO)_4Hg$ $Co(CO)_4$	1.310	44.766	31.69	58.46	134.908	-do-	-do-	42.085	43.863	-do-	-do-	48.18	54.142
$Fe_2(CO)_9$	1.707	43.568	30.52	57.97	132.052	0.889	0.889	48.694	50.471	0.889	0.889	53.91	59.866
$*Co_2(CO)_8$	1.433	43.382	32.35	50.67	126.387	-do-	-do-	41.265	43.042	-do-	-do-	46.16	52.121
$**Co_2(CO)_8$	1.384	43.382	33.84	43.63	120.844	-do-	-do-	38.965	40.742	-do-	-do-	38.64	44.604

*Possesses both terminal and bridging CO groups. ** Possesses only terminal CO groups

Table: 4 .σ, δ values [p pm] of M, C & O in Bi-nuclear Carbonyls [a]

Carbonyl [Fig. No.]	M ADF No.	δ M [3]	σ M	ADF Nos. of C	δ ^{13}C [2]	σ^{13} C	ADF Nos. of O	δ^{17} O [3]	σ^{17} O
$Mn_2(CO)_{10}$ (1)	1,2	3672.1	-3672.1	(3,5,7,11,13, 15, 19,21) [9,17]	(221.0) [196.33]	(-39.9) [-15.23]	(4,6,8,12,14,16, 20, 22) [10,18]	(113.5) [49.7]	(-113.5) [-49.67]
$Tc_2(CO)_{10}$ (2)	1,2	35.1	-35.1	(3,5,7,9,13,15, 17,19) [11,21]	(208.7) [177.04]	(-27.6) [4.06]	(4,6,8,10,14,16, 18,20) [12,22]	(92.6) [22.2]	(-92.6) [-22.2]
$Re_2(CO)_{10}$ (3)	1,2	-3029.8	3029.8	(3,5,7,9,12, 13,15,19) [17,21]	(204.1) [174.80]	(-23.0) [6.3]	(4,6,8,10,11,14, 16, 20) [18,22]	(84.2) [21.3]	(-84.2) [-21.27]
$Co(CO)_4Zn$ $Co(CO)_4$ (4)	Zn(1) Co(2,3)	-2260.9 4134.3	2260.9 -4134.3	(4,6,8,10, 12,14) [17,18]	(189.1) [208.4]	(-8.0) [-27.3]	(5,7,9,11, 13,15) [16,19]	(51.4) [100.0]	(-51.4) [-100.0]
$Co(CO)_4Cd$ $Co(CO)_4$ (5)	Cd(1) Co(2,3)	-4381.4 4139.3	4381.35 -4139.3	(4,8,10,14, 16,18) [6,12]	(189.5) [208.3]	(-8.4) [-27.2]	(5,9,11,15, 17,19) [7,13]	(54.9) [99.1]	(-54.9) [-99.1]
$Co(CO)_4Hg$ $Co(CO)_4$ (6)	Hg(1) Co(2,3)	-7202.3 4184.8	7202.30 -4184.8	[4,8,12,14, 16,18) [6,10]	(189.3) [209.7]	(-8.2) [-28.6]	(5,9,13,15, 17,19) [7,11]	(55.6) [102.1]	(-55.6) [-102.1]
$Fe_2(CO)_9$ (7)	1,14	-3566.1	3566.1	(2,4,6,12, 16 ,19) T [9,10,11] B	(192.2) [266.8]	(-11.1) [-85.7]	(3,5,7,13, 15,20) [8,17,18]	(60.0) [355.1]	(-60.0) [-355.1]
$Co_2(CO)_8$ Bgd (8)	1,2	4796.5	-4796.5	(3,5) B [7,15] T-1 {10,11,13,17} T-2	(298.4) [174.3] {198.2}	(-117.3) [6.79] {-17.1}	(4,6) [8,16] {9,12,14,18}	(539.2) [16.8] {77.7}	(-539.2) [-16.8] {-77.7}
$Co_2(CO)_8$ Ter (9)	1 b 2 c	5089.1 5130.1	-5089.1 -5130.1	(3,9,13,15) T-I [5,7,11,17] T-II	(215.0) (198.0)	(-33.9) [-16.9]	(4,10,14,16) [6,8,12,18]	(122.3) [59.6]	(-122.3) [-59.6]

a. ADF Numbers in parentheses(hold good in all tables for figures);For relations:2, 3, see 4.1. **b** and **c:** differ slightly; **B**= Bridging ; **T**= Terminal; **T-I** Terminal of first type **T-II** Terminal of second type

Table: 5. Shielding Constants [p pm] of M, Diamagnetic and Paramagnetic Contributions

Carbonyl	σ M (MCO)	Diamagnetic contributions {a} {b}	Paramagnetic contributions {c} {d} {e} {f}
$Mn_2(CO)_{10}$	Mn(1,2)-3672.1	1825.325, 99.928	-230.076,-6280.745,925.163,-11.665
$Tc_2(CO)_{10}$	Tc(1,2) -35.1	4048.887 ,76.849	-812.474,-4755.560,1415.083,-7.886
$Re_2(CO)_{10}$	Re(1,2) 3029.8	8670.042 217.460	629.867,-6238.834, -241.885, -6.860
$Co(CO)_4Zn$ $Co(CO)_4$	Zn(1) 2260.9 Co(2,3)-4134.3	2234.153, 283.613 1989.204, 168.250	-40.466,-209.198, -14.948, 7.692 -166.554,-6807.818, 683.672, -1.098
$Co(CO)_4Cd$ $Co(CO)_4$	Cd(1) 4381.35 Co(2,3) -4139.3	4613.823 ,201.950 1989.204 ,168.098	-86.918 , -294.597 -61.413 , 8.502 -159.022 ,-6821.714, 683.825, 0.335
$Co(CO)_4Hg$ $Co(CO)_4$	Hg(1) 7202.30 Co(2,3)-4184.8	9377.948 ,349.258 1989.204 ,168.085	120.234,-2068.537,-585.275, 8.671 -154.329, -6870.088, 681.589, 0.784
$Fe_2(CO)_9$	Fe(1,14)-3566.1	1907.276 ,131.123	-248.370,-5874.991, 521.495 -2.655
$Co_2(CO)_8$ Bgd	Co(1,2)-4796.5	1989.202 ,168.175	-200.107,-7221.069,469.827,-2.559
$Co_2(CO)_8$ Ter	Co(1) b -5089.1 Co(2) c -5130.1	1989.202 ,167.072 1989.110 167.181	-166.084,-7843.494,767.393 ,-3.183 -179.110,-7928.691, 828.553 -7.135

For {a}, {b},{c}, {d},{e},{f} see Introduction. This also holds good in tables-6,7.

Table: 6. Shielding Constants [p pm] of ^{13}C, Diamagnetic, and Paramagnetic Contributions

Carbonyl	σ ^{13}C(MCO)	Diamagnetic contributions {a} {b}	Para magnetic contribution {c} {d} {e} {f}
$Mn_2(CO)_{10}$	C(3,5,7,11,13,15,19,21)-39.9 C(9,17) -15.23	199.227, 49.133. -do- , 48.983	1.045 ,-322.682, 31.115,2.226 -2.781,-290.302,31.178 ,-1.495
$Tc_2(CO)_{10}$	C(3, 5,7,9,13,15,17,19) -27.6 C(11,21) 4.06	-do- , 49.557 -do- , 49.55	1.161 ,-307.557, 26.766, 3.285 -2.745 ,-277.590, 36.288, -0.77
$Re_2(CO)_{10}$	C(3,5,7,9,12,13,15,19)-22.97 C(17,21) 6.3	-do- , 50.743 -do- , 49.540	0.594 ,-305.543, 29.172 , 2.844 -0.868,-278.095, 38.831,-2.128
$Co(CO)_4Zn$ $Co(CO)_4$	C(4,6,8,10,12,14) -8.04 C(17,18) -27.32	-do- , 51.189 -do- , 51.224	1.435, -300.114,37.594, 2.500 -3.931,-296.765, 24.694,-1.767
$Co(CO)_4Cd$ $Co(CO)_4$	C(4,8,10,14,16,18) -8.43 C(6,12) -27.23	-do- , 51.227 -do- , 51.292	1.511,-301.398,38.186,2.859 -4.143,-296.858, 25.061,-1.806
$Co(CO)_4Hg$ $Co(CO)_4$	C(4,8,12,14,16,18) -8.20 C(6,10) -28.57	-do- , 51.329 -do- , 51.287	1.512 , -301.788 ,38.843, 2.679 -4.171,-298.366, 25.294,-1.839
$Fe_2(CO)_9$	C(2,4,6,12,16,19) -11.14 C(9,10,11) -85.73	199.227, 48.893 -do- , 44.555	1.035, -286.395, 26.748, -0.931 3.634, -394.424, 71.397, -10.113
$Co_2(CO)_8$ Bgd	C(3,5) -117.55 C(7,15) 6.79 C(10,11,13,17)-17.12	-do- , 47.660. -do- , 50.119 -do- , 50.322	2.635, -416.397, 51.965, -2.642 -0.803, -271.308, 28.137,1.416 -0.061 ,-298.777, 32.135, 0.033
$Co_2(CO)_8$ Ter	C(3,9,13,15) -33.82 b C(5,7,11,17) -16.95 c	-do- , 51.123 -do- , 50.268	1.343 , -320.407 ,32.825,2.070 -0.307,-301.561, 35.212 ,0.209

Table: 7. Shielding Constants [p pm] of ^{17}O, Diamagnetic and Paramagnetic Contributions

Carbonyl	**σ ^{17}O (MCO)**	**Diamagnetic contribution** {a} {b}	**Paramagnetic contributions** {c} {d} {e} {f}
$Mn_2(CO)_{10}$	O(4,6,8,12,14,16,20,22) -113.5 O(10,18)-49.67	269.472, 130.346 269.472,130.346	0.801,-471.988,-40.845,-1.317 -1.461,-394.994,-50.389,-2.676
$Tc_2(CO)_{10}$	O(4, 6,8,10,14,16,18,20)-92.6 O(12,22) -22.21	269.472 ,130.355 269.472 ,130.901	0.839,-448.130,-44.148,-0.954 -1.502,-366.832,-52.152,-2.098
$Re_2(CO)_{10}$	O(4,6,8,10,11,14,16,20))-84.2 O(18,22) -21.27	269.472 ,130.187 269.471 ,130.203	0.594,-452.543,-29.172,-2.844 -0.617,-371.712,-46.177,-2.436
$Co(CO)_4Zn$ $-Co(CO)_4$	O(5,7,9,11,13,15) -51.40 O(16,19) -100.01	269.469 ,130.532 269.467 ,129.831	1.193,-411.635,-41.558,0.585 -2.031,-447.866,-46.936,-2.475
$Co(CO)_4$ $Cd\ Co(CO)_4$	O(5,9,11,15,17,19) -54.85 O(7,13) -99.05	269.469 ,130.862 269.468 ,129.838	1.340,-411.718,-45.134 , 0.331 -2.133,-446.204,-47.546,-2.473
$Co(CO)_4$ $Hg\ Co(CO)_4$	O(5,9,13,15,17,19) -55.62 O(7,11) -102.10	269.469. 130.857 269.468 ,129.898	1.370 ,-412.112,-45.472,0.240 -2.146,-449.093,-47.752,-2.469
$Fe_2(CO)_9$	O(3,5,7,13,15,20) -60.00 O(8,17,18) -355.10	269.468 ,129.630 269.468 ,134.00	-0.489,-419.139,-38.496,-1.010 1.035,-786.395,26.748,-0.931
$Co_2(CO)_8$ Bgd	O(4,6)) -539.18 O(8,16) -16.81 O(9,12,14,18) -77.70	269.468 ,133.05 269.472 ,130.220 269.472 ,129.885	1.316 ,-842.290,-98.080,-2.646 -0.372,-373.482,-42.395,-0.252 0.061,-435.472, -40.597 -1.051
$Co_2(CO)_8$ Ter	O(4,10,14,16) -122.31 b O(6,8,12,18) -59.60 c	269.472 ,129.903 269.472 ,129.462	0.958,-487.472, -34.760,-0.407 -0.025,-410.917,-48.004,-0.575

Table: 8. Total Diamagnetic and Paramagnetic Contributions in σ M, σ^{13} C and σ^{17} O [p pm]

Carbonyl	M ADF No	Dia. Cont.	Para. Cont.	ADF No. of C	Dia. Cont.	Para. Cont.	ADF No .of O	Dia. Cont.	Para. Cont.
$Mn_2(CO)_{10}$	1,2	1925.25	-5597.32	(3,5,7,11,13, 15, 19,21) [9,17]	(248.36) [248.21]	(-288.3) [-263.4]	(4,6,8,12,14, 16, 20, 22) [10,18]	(399.82) [399.85]	(-513.345) [-449.520]
$Tc_2(CO)_{10}$	1,2	4125.74	-4160.84	(3,5,7,9,13,15, 17,19) [11,21]	(248.784) [248.78]	(-276.3) [-244.8]	(4,6,8,10,14, 16, 18,20) [12,22]	(399.83) [400.37]	(-492.41) [-422.584]
$Re_2(CO)_{10}$	1,2	8887.50	-5857.72	(3,5,7,9,12, 13, 15,19) [17,21]	(249.97) [248.668]	(-272.9) [-242.4]	(4,6,8,10,11, 14, 16, 20) [18,22]	(399.66) [399.67]	(-483.814) [-420.942]
$Co(CO)_4Zn$ $Co(CO)_4$	Zn(1) Co(2,3)	2517.77 2157.45	-256.920 -6291.80	(4,6,8,10, 12,14) [17,18]	(250.416) [250.451]	(-258.5) [-277.8]	(5,7,9,11, 13,15) [16,19]	(400.00) [399.30]	(-451.414) [-499.308]
$Co(CO)_4Cd$ $Co(CO)_4$	Cd(1) Co(2,3)	4815.77 2157.30	-434.426 -6296.58	(4,8,10,14, 16,18) [6,12]	(250.454) [250.519]	(-258.8) [-277.7]	(5,9,11,15, 17,19) [7,13]	(400.33) [399.31]	(-455.181) [-498.356]
$Co(CO)_4Hg$ $Co(CO)_4$	Hg(1) Co(2,3)	9727.21 2157.29	-2524.91 -6342.04	[4,8,12,14, 16,18) [6,10]	(250.556) [250.514]	(-258.8) [-279.1]	(5,9,13,15, 17,19) [7,11]	(400.33) [399.37]	(-455.973) [-501.460]
$Fe_2(CO)_9$	1,14	2038.40	-5604.52	(2,4,6,12,16 ,19) **T** [9,10,11] **B**	248.612 243.782	-259.8 -329.5	(3,5,7,13, 15,20) [8,17,18]	399.10 403.47	-459.026 -758.544
$Co_2(CO)_8$ Bgd	1,2	2157.38	-6953.91	(3,5) **B** [7,15] **T** {10,11,13,17} **T**	246.888 249.345 249.549	-364.2 -242.6 -266.7	(4,6) [8,16] (9,12,14,18)	402.52 399.69 399.36	-942.00 -416.501 -477.059
$Co_2(CO)_8$ Ter	1 b 2 c	2156.27 2156.26	-7245.37 -7286.38	(3,9,13,15) **T-I** [5,7,11,17]**T-II**	250.35 249.495	-284.2 -266.5	(4,10,14,16) [6,8,12,18]	399.37 399.93	-521.602 -459.521

T=Terminal; **B**= Bridging**; T-I, T_2** Terminal of first and second type, **Dia. Cont. = Diamegnetic contribution, Para. Cont. = Paramagnetic contribution.**

Table: 9. Spatial Classification of Metals & CO Ligands

Carbonyls	**Types of σM**	**Types of σ ^{13}C & σ ^{17}O**	**No of spatially different M & CO**
$Mn_2(CO)_{10}$	One	Two each	Same type of metals ;2 types of CO; 8 of one type & 2 of other type
$Tc_2(CO)_{10}$	-do-	-do-	-do-
$Re_2(CO)_{10}$	-do-	-do-	-do-
$Co(CO)_4ZnCo(CO)_4$	One	-do-	Same type of metals; 2 types of O; 6 of one type & 2 of other type
$Co(CO)_4CdCo(CO)_4$	-do-	-do-	-do-
$Co(CO)_4HgCo(CO)_4$	-do-	-do-	-do-
$Fe_2(CO)_9$	-do-	-do-	Both Metals of same type; 2 types of C ; 6 of one type & 3 of other type
$Co_2(CO)_8$ Bdg.	-do-	Three each	Both Metals of same type;2 types of C; 6 of one type & 2 of other type
$Co_2(CO)_8$ Ter.	Two	Two each	Both Metals of different types ; 2 types of C;4 of each type

Table: 10.σ ^{13}C [p pm] of C Bonded to 1st and 2nd Metal

Carbonyl	Spatially Equivalent C with σ ^{13}C [a]	C atoms bonded to [a]	
		1st Metal	2nd Metal
$Mn_2(CO)_{10}$	C(3,5,7,11,13,15,19, 21) = -39.9 C(9,17) = -15.23	(13,15,19,21) **T-1** (17)**T-1**	(3,5,7,11) **T-1** (9) **T-2**
$Tc_2(CO)_{10}$	C(3, 5,7,9,13,15,17,19) -27.6 C(11,21) 4.06	(3,5,7,9)**T-1** (11) **T-2**	(13,15,17,19) **T-1** (21) **T-2**
$Re_2(CO)_{10}$	C(3,5,7,9,12,13,15,19)-22.97 C(17,21) 6.3	(12,13,15,19) **T-1** (17) **T-2**	(3,5,7,9) **T-1** (21) **T-2**
$Co(CO)_4$ Zn $Co(CO)_4$	C(4,6,8,10,12,14)-8.04 C(17,18) =-27.32	(10,12,14) **T-1** (17) **T-2**	(4,6,8) **T-1** (18) **T-2**
$Co(CO)_4$-Cd $Co(CO)_4$	C(4,8,10,14,16,18)-8.43 C(6,12)= -27.23	(10,14,18) **T-1** (12) **T-2**	(4,8,16) **T-1** (6) **T-2**
$Co(CO)_4$Hg Co $(CO)_4$	C(4,8,12,14,16,18)-8.20 C(6,10)= -28.57	(12,14,18) **T-1** (10) **T-2**	(4, 8,16) **T-1** (6) **T-2**
$Fe_2(CO)_9$	C(2,4,6,12,16,19)-11.14 C(9,10,11)= -85.73	(2,4,6) **T** (9,10,11) **B**	(12,16,19) **T** (9,10,11) **B**
$Co_2(CO)_8$ Bgd	C(7,15) 6.79 C(10,11,13,17) -17.12 C(3,5)= -117.55	(7) **T** (11,17) **T** (3,5) **B**	(15) **T** (10,13) **T** 3,5 **B**
$Co_2(CO)_8$ Ter.	C(3,9,13,15) -33.82 C(5,7,11,17) -16.95	(3,9) **T-I** (5,7) T-**II**	(13,15) **T-I** (11,17) T-**II**

T-1 and **T-2** =Terminal of first and second types. **B**= Bridging

Table: 11. k, j & H^{spin} Values of Nuclei in Bi-nuclear Carbonyls

Perturbing nucleus	Responding Nuclei[a]	k [10^{19} kg m^{-2} s^{-2} A^{-2}]	j (p pm)	H^{spin} (10^{17} MHz mol^{-1})
$Mn_2(CO)_{10}$				
Mn(1)	Mn (2) C(3,5,7,11) C(9) C(13,15,19,21) C(17)	209.004 -3.987 -12.462 380.824 293.770	152.805 -2.983 -9.288 283.837 218.954	5752.153 -21.480 -69.627 2136.938 1648.450
Mn(2)	Mn (1) C(3,5,7,11) C(9) C(13,15,19,21) C(17)	209.004 380.330 293.673 -3.998 -12.549	152.805 283.470 218.882 -2.980 -9.353	5752.153 2136.938 1648.450 -22.436 -70.416
$Tc_2(CO)_{10}$				
Tc(1)	Tc (2) C(3,5,7,9) C(11) C(13,15,17,19) C(21)	753.021 697.422 389.311 -9.004 -51.291	0.000 0.000 0.000 0.000 0.000	 *
Tc (2)	Tc (1) C(3,5,7,9) C(11) C(13,15,17,19) C(21)	753.021 -9.004 -51.291 697.422 389.310	0.000 0.000 0.000 0.000 0.000	 *
$Re_2(CO)_{10}$				
Re(1)	Re(2) C(3,5,7,9) C(12,13,15,19) C(17) C(21)	-617.847 -5.096 546.030 299.962 -89.796	0.000 0.000 0.000 0.000 0.000	 * *
Re(2)	Re(1) C(3,5,7,9) C(12,13,15,19) C(17) C(21)	-617.847 546.071 -5.097 -89.796 299.914	0.000 0.000 0.000 0.000 0.000	 * *
$Co(CO)_4$-Zn-$Co(CO)_4$				
Zn(1)	Co(2,3) C(4,6,8,10,12,14) C(17,18)	1687.779 -335.618 -62.027	300.057 -63.552 -11.745	15813.379 -478.467 -88.425
Co(2)	Zn(1) Co(3) C(4,6,8) C(10,12,14) C(17) C(18)	1687.786 -92.142 21.099 721.729 571.570 0.896	300.058 -61.713 15.051 514.857 407.739 0.639	15813.379 -4553.293 158.641 5426.721 4297.671 6.735
Co(3)	Zn(1)	1687.786	300.058	15813.379

	Co(2)	-92.142	-61.713	-4553.293
	C(4,6,8)	721.729	514.857	5426.721
	C(10,12,14)	21.099	15.051	158.641
	C(17)	0.896	0.639	6.735
	C(18)	571.571	407.739	4297.671
$Co(CO)_4$-Cd-$Co(CO)_4$				
Cd(1)	Co(2,3)	5487.882	464.923	-36521.547
	C(4,8,10,14,16,18)	-1081.242	727.12	1094.861
	C(6,12)	-330.195	222.051	2340.473
Co(2)	Cd(1)	5487.884	3464.92 -	-36521.547
	Co(3)	-175.019	117.220	-8648.697
	C(4,8,16)	38.759	27.649	291.427
	C(6)	10.732	7.656	80.696
	C(10,14,18)	714.648	509.806	5373.482
	C(12)	636.999	454.41	4789.595
Co(3)	Cd (1)	5487.787	-464.864	-36520.533
	Co(2)	-175.019	-117.220	-8648.697
	C(4,8,16)	714.626	509.790	5373.314
	C(6)	636.998	454.413	4789.626
	C(10,14,18)	38.759	27.649	291.427
	C(12)	10.734	7.657	80.707
$Co(CO)_4$-Hg-$Co(CO)_4$				
Hg(1)	Co(2,3)	9477.03	4869.057	51321.078
	C(4,8,12,14,16,18)	-2308.414	-1263.225	-13314.707
	C(6,10)	-901.92	-493.554	-5202.183
Co(2)	Hg(1)	9477.031	4869.057	51321.078
	Co(3)	-222.094	-148.749	-10974.962
	C(4,8,16)	51.223	36.541	385.151
	C(6)	18.392	13.120	138.289
	C(10)	644.495	459.761	4845.996
	C(12,14,18)	719.882	513.539	5412.829
Co(3)	Hg(1)	9477.031	4869.057	51321.078
	Co(2)	-222.094	-148.749	-10974.962
	C(4,8,16)	719.885	513.542	5412,900
	C(6)	644.503	459.766	4846.100
	C(10)	18.388	13.118	138.270
	C(12,14,18)	51.221	36.540	385.147
$Fe_2(CO)_9$				
Fe(1)	C(2,4,6)	558.847	54.527	82.104
	C(9,10,11)	248.911	24.286	36.569
	C(12, 16,19)	-3.562	-0.348	-0.524
	Fe(14)	240.066	3.008	4.529
Fe(14)	Fe(1)	240.066	3.008	4.529
	C(2,4,6)	-3.553	-0.347	-0.522
	C(9,10,11)	249.021	24.297	36.585
	C(12,16,19)	558.917	54.533	82.113
$Co_2(CO)_{8\ Bgd.}$				
Co(1)	Co(2)	213.246	142.823	10537.731
	C(3,5)	382.744	273.037	2877.878
	C(7)	904.613	645.321	6801.845
	C(10,13)	-37.387	-26.671	-281.119
	C(11,17)	504.505	359.897	3793.404
	C(15)	41.864	29.864	314.774
Co(2)	Co(1)	213.246	142.823	10537.731
	C(3,5)	382.744	273.037	2877.878
	C(7)	41.864	29.864	314.774
	C(10,13)	504.506	359.897	3793.404
	C(11,17)	-37.388	-26.671	-281.109
	C(15)	904.613	645.320	6801.845
$Co_2(CO)_{8\ Ter.}$				
Co(1)	Co(2)	289.764	194.072	14318.972
	C(3,9)	655.425	467.558	4928.178
	C(5,7)	611.741	436.395	4599.712
	C(11,13,17)	-0.539	-0.384	-4.047
	C(15)	-0.090	-0.064	-0.675
Co(2)	Co(1)	289.764	194.072	14318.972
	Co(3,7)	0.053	0.038	0.401
	C(5)	-0.414	-0.295	-3.109
	C(9)	0.340	0.243	2.561
	C(11,17)	611.782	436.425	4500.029
	C(13,15)	654.935	467.208	4924.489

*Radioactive ^{99}Tc remained uncoupled **Large difference of γ in ^{187}Re (0.23057) and γ ^{13}C (6.7383) prohibits spin- spin interaction. **a**. ADF numbers in parentheses [See Figs: 1-9]

Table: 12. Designation of IR/Raman Bands* and Their Vibration Symmetry Classes

Carbonyl	Vibration Symmetries of bands	IR-active bands	Raman-active bands	Both IR- and Raman active bands	IR inactive bands	May not be Raman observed bands [a]	Vibration Symmetry Class
$M_2(CO)_{10}$ (M=Mn, Tc, Re) $[D_{4d}]$	A_1	---	$A_1(7)$	---	$A_1(7)$	---	$[7A_1+A_2+2B_1+6B_2+8E_1+6E_2+8E_3]$
	A_2	---	$A_2(1)$	---	$A_2(1)$	$A_2(1)$	
	B_1	---	$B_1(2)$	---	$B_1(2)$	$B_1(2)$	
	B_2	$B_2(6)$	$B_2(6)$	$B_2(6)$	----	$B_2(6)$	
	E_1	$E_1(16)$	$E_1(16)$	$E_1(16)$	----	$E_1(16)$	
	E_2	---	$E_2(12)$	----	$E_2(12)$	---	
	E_3	---	$E_3(16)$	---	$E_3(16)$	----	
$Co(CO)_4$ –M-$Co(CO)_4$ (M=Zn, Cd , Hg) $[D_{3d}]$	A_{1g}	---	$A_{1g}(7)$	---	$A_{1g}(7)$	---	$[7A_{1g}+A_{2g}+2A_{1u}+7A_{2u}+8E_{1g}+9E_{1u}]$
	A_{2g}	---	$A_{2g}(1)$	----	$A_{2g}(1)$	$A_{2g}(1)$	
	A_{1u}	----	$A_{1u}(2)$	----	$A_{1u}(2)$	$A_{1u}(2)$	
	A_{2u}	$A_{2u}(7)$	$A_{2u}(7)$	$A_{2u}(7)$	----	$A_{2u}(7)$	
	E_{1g}	----	$E_{1g}(16)$	----	$E_{1g}(16)$	----	
	E_{1u}	$E_{1u}(18)$	$E_{1u}(18)$	$E_{1u}(18)$	----	$E_{1u}(18)$	
$Fe_2(CO)_9$ $[D_{3h}]$ Three bridging & six terminal COs	$AA_1(7)$	----	$AA_1(7)$	----	$AA_1(7)$	----	$[7AA_1+3AA_2+2AAA_1+6AAA_2+10EE_1+8EEE_3]$
	$AA_2(3)$	-----	$AA_2(3)$	----	$AA_2(3)$	$AA_2(3)$	
	$AAA_1(2)$	-----	$AAA_1(2)$	----	$AAA_1(2)$	$AAA_1(2)$	
	$AAA_2(6)$	$AAA_2(6)$	$AAA_2(6)$	$AAA_2(6)$	----	$AAA_2(6)$	
	$EE_1(20)$	$EE_1(20)$	$EE_1(20)$	$EE_1(20)$	----	----	
	$EEE_1(16)$	----	$EEE_1(16)$	----	$EEE_1(16)$	----	
$Co_2(CO)_8$ $[C_{2v}]$ Two bridging & six terminal COs	A_1	$A_1(15)$	$A_1(15)$	$A_1(15)$	----	----	$[15A_1+10A_2+11B_1+12B_2]$
	A_2	---	$A_2(10)$	----	$A_2(10)$	-----	
	B_1	$B_1(11)$	$B_1(11)$	$B_1(11)$	---	----	
	B_2	$B_2(12)$	$B_2(12)$	$B_2(12)$	-----	-----	
$Co_2(CO)_8$ $[D_{3d}]$ All terminal COs	A	A(48)	A(48)	A(48)	---	----	[48A]

*Numbers in parentheses indicate bands . **a**. Raman active; but intensity being [10-29 to-30]; were not observed.

Table: 13. Bond Lengths and Bond Strengths in $[M_2(CO)_{10}]$(M= Mn,Tc, Re)

Carbonyl	S_{MM} kJ mol^{-1}	d_{M-M} (A^0)
$[Mn_2(CO)_{10}]$ [26-29]	154.8	2.94
$[Tc_2(CO)_{10}]$ [26-29]	188.3	3.04
$[Re_2(CO)_{10}]$] [26-29]	221.7	3.04

Table: 14. Wave Numbers and Total Coordination Shifts in $[M_2(CO)_{10}]$ (M= Mn, Tc, Re)

Carbonyl	ν_{CO} [IR (cm^{-1})]	Total coordination shift($\Delta\ \delta^{13}C_T$)[p pm]
$[Mn_2(CO)_{10}]$	**2044**, 2013,1983 [26-29]	-5.21=[(-39.9+34.44)*8+(-15.23+34.44)*2]
$[Tc_2(CO)_{10}]$	**2065**,2017,1984 [26-29]	131.72=[(-27.6+34.44)*8+(4.06+34.44)*2]
$[Re_2(CO)_{10}]$	**2070**, 2017,1984 [26-29]	173.00=[(-23.0 +34.44)*8 +(6.3 +34.44)*2]

Table: 15. Wave Numbers and Total Coordination Shifts in M $[Co(CO)_4]_2$(M= Zn, Cd , Hg)

Carbonyl	$\Delta\ \delta^{13}C$ [p pm]	ν_{CO} [Raman(cm^{-1})]	ν_{CO} [IR(cm^{-1})]
$Zn[Co(CO)_4]_2$	172.68= [(-8.04+34.44)*6+(-27.3+34.44)*2]	≈2107-2115[37]	≈2032-2040[38]
$Cd\ [Co(CO)_4]_2$	170.72=[(-8.4+34.44)*6+(-27.2+34.44)*2]	≈2030-*2040* [37]	≈2022-2030[38]
$Hg[Co(CO)_4]_2$	169.12= [(-8.2+34.44)*6+(-28.6+34.44)*2]	≈*1990-2000* [37]	≈2007-2015[38]

Table: 16. Wave numbers and Shielding Constants of $[Fe_2(CO)_9]$ and [Brgd& Ter $Co_2(CO)_8$]

Carbonyl	$\sigma^{13}C$ terminal ($\sigma^{17}O$ terminal)	$\sigma^{13}C$ bridged ($\sigma^{17}O$ bridged)	ν_{CO}terminal (cm^{-1})	ν_{CO}bridged (cm^{-1})	d_{M-M} (A^0)
$[Fe_2(CO)_9]$	-11.14 (-60.00)	-85.73 (-355.10)	2080,2034[37]	1828	2.46
Bridged $[Co_2(CO)_8]$	6.79, -17.12 (-16.81, -77.70)	-117.55 (-539.18)	2075,2064[25] 2047,2035,2028	1867 1859	1.90
Terminal $[Co_2(CO)_8]$	-33.82, -16.95 (-122.31, -59.60)	----	2107, 2069[38] 2042 , 2031 2023, 1991	----	1.8

Captions for Figures:

Fig.1. D_{4d} stereochemistry of $[Mn_2(CO)_{10}]$
Fig.2. D_{4d} stereochemistry of $[Tc_2(CO)_{10}]$
Fig.3. D_{4d} stereochemistry of $[Re_2(CO)_{10}]$
Fig.4. D_{3d} stereochemistry of $[Co(CO)_4$-Zn-$Co(CO)_4]$
Fig.5. D_{3d} stereochemistry of $[Co(CO)_4$-Zn-$Co(CO)_4]$
Fig.6. D_{3d} stereochemistry of $[Co(CO)_4$-Zn-$Co(CO)_4]$
Fig.7. D_{3h} stereochemistry of $[Fe_2(CO)_9]$
Fig.8. D_{2d} stereochemistry of terminal $[Co_2(CO)_8]$
Fig.9. C_{2v} stereochemistry of bridged $[Co_2(CO)_8$

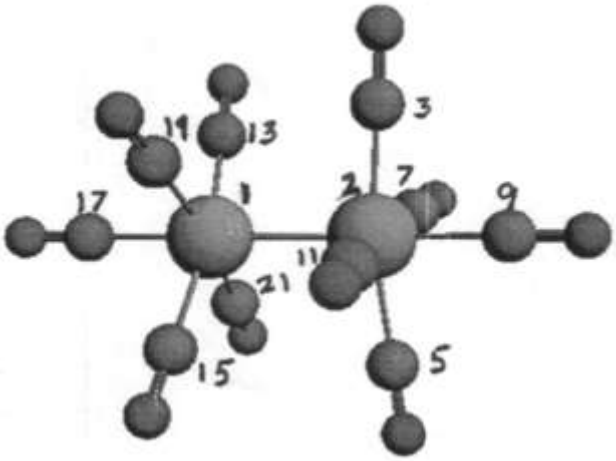

Fig.1. D_{4d} stereochemistry of $[Mn_2(CO)_{10}]$

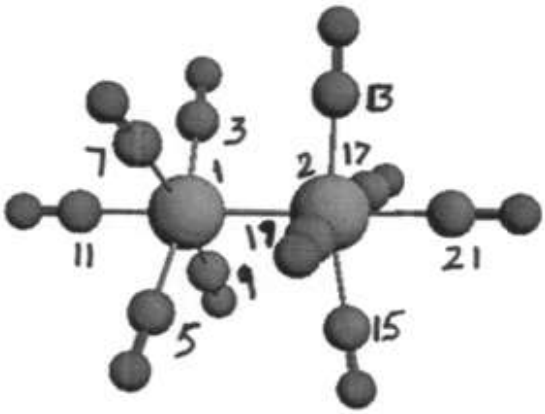

Fig .2. D_{4d} stereochemistry of $[Tc_2(CO)_{10}]$

Fig.3. D_{4d} stereochemistry of $[Re_2(CO)_{10}]$

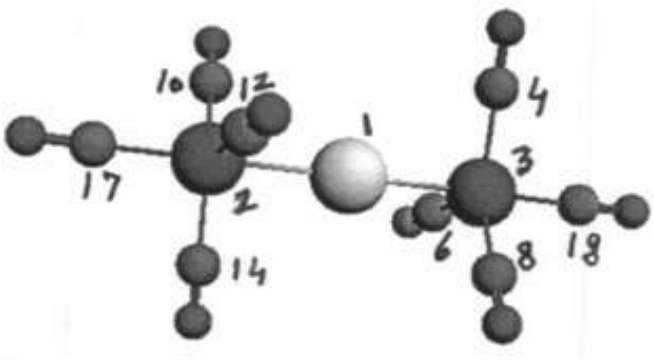

Fig.4. D_{3d} stereochemistry of $[Co(CO_{4}–Zn–Co(CO)_4]$

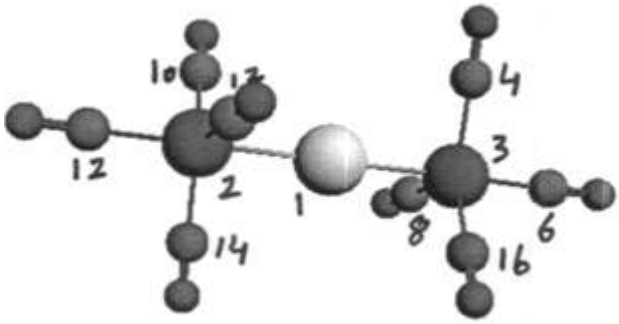

Fig. 5. D_{3d} stereochemistry of $[Co(CO)_4–Cd–Co(CO)_4]$

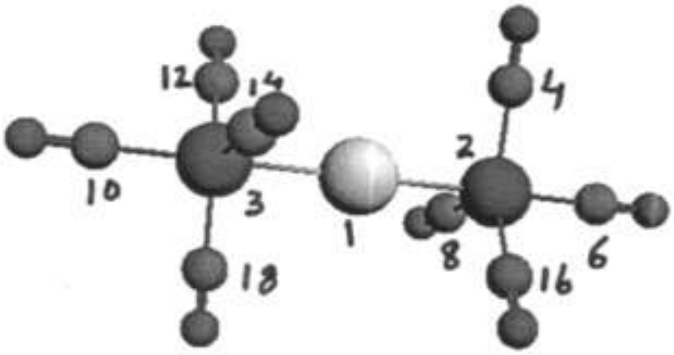

Fig.6. D_{3d} stereochemistry of $[Co(CO)_4–Hg–Co(CO)_4]$

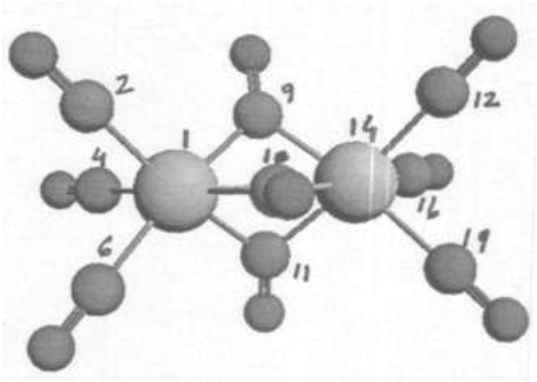

Fig.7. D_{3h} stereochemistry of $[Fe_2(CO)_9]$

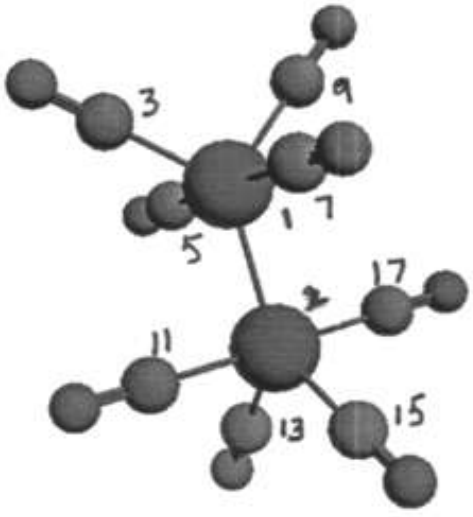

Fig.8. D_{2d} stereochemistry of terminal $[Co_2(CO)_8]$

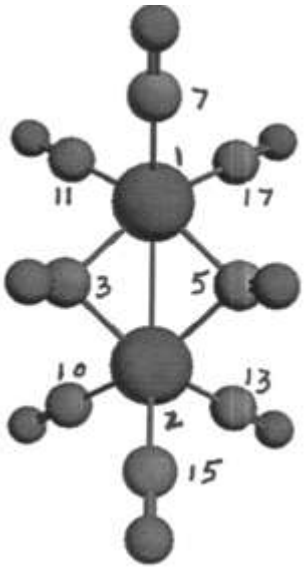

Fig.9 C_{2v} stereochemistry of bridged $[Co_2(CO)_8]$

Refrences

[1] Holmes, N. J.; Levason, W.; Webster, M. Triphenylstibine substituted manganese and rhenium carbonyls: synthesis and multinuclear NMR spectroscopic studies. X-ray crystal structures of ax-$[Mn_2(CO)_9(SbPh_3)]$, $[Mn(CO)_5(SbPh_3)][CF_3SO_3]$ and fac-$[Re(CO)_3Cl(SbPh_3)_2]$. *J. Organomet. Chem.* **1998,** 568, 213-223.

[2] Jia, R.; Wang, C.; Qiong, L.; Li, Q.-S.; Xie, Y.; King, R. B.; Schaefer, H. F. Major Differences Between Mononuclear and Binuclear Manganese Carbonyl Cyanides and Isoelectronic Binary Chromium Carbonyls Arising from Basicity of the Cyanide Nitrogen Atom*. *Aus. J. Chem.* **2014,** 67, 1318-1323.

[3] Zeng, Y.; Wang, S.; Feng, H.; Xie, Y.; King, R. B. Highly Unsaturated Binuclear Butadiene Iron Carbonyls: Quintet Spin States, Perpendicular Structures, Agostic Hydrogen Atoms, and Iron-Iron Multiple Bonds. *Int. J. Mol. Sci.* **2011,** 12, 2216.

[4] Xu, B.; Li, Q.; Xie, Y.; King, B.; Schaefer III, H. Heptacarbonyldiosmium and Hexacarbonyldiosmium: Two Highly Unsaturated Binuclear Osmium Carbonyls. *Croatica. chemica. acta.* **2009,** 82, 207-218.

[5] Xu, B.; Li, Q.-S.; Xie, Y.; King, R. B.; Schaefer, H. F. Homoleptic Mononuclear and Binuclear Osmium Carbonyls $Os(CO)_n$(n = 3−5) and $Os_2(CO)_n$ (n = 8, 9): Comparison with the Iron Analogues. *Inorg. Chem.* **2008,** 47, 3869-3878.

[6] Ehlers, A. W.; Frenking, G. Structures and Bond Energies of the Transition Metal Hexacarbonyls $M(CO)_6$ (M = Cr, Mo, W). A Theoretical Study. *J. Am. Chem. Soc.* **1994,** 116, 1514-1520.

[7] Delley, B.; Wrinn, M.; Lüthi, H. P. Binding energies, molecular structures, and vibrational frequencies of transition metal carbonyls using density functional theory with gradient corrections. *J. Chem. Phys.* **1994,** 100, 5785-5791.

[8] Carreon-Macedo, J.-L.; Harvey, J. N. Computational study of the energetics of $3Fe(CO)_4$, $1Fe(CO)_4$ and $1Fe(CO)_4(L)$, L = Xe, CH_4, H_2 and CO. *Phys. Chem. Chem. Phys.* **2006,** 8, 93-100.

[9] Niu, S.; Hall, M. B. Theoretical Studies on Reactions of Transition-Metal Complexes. *Chem. Rev.* **2000,** 100, 353-406.

[10] Sizova, O. V.; Varshavskii, Y. S.; Nikol'skii, A. B. Binuclear Rhodium(I) Carbonyl Carboxylate Complexes: DFT Study of Structural and Spectral Properties. *Russ. J. Coord. Chem.* **2005,** 31, 875-883.

[11] Luo, Q.; Li, Q.-S. DFT Studies on Unsaturated Ruthenium Carbonyls-heptacarbonyldiruthenium and Hexacarbonyldiruthenium. *Chem. J. Chines. Uni.* **2008,** 29, 2430-2434.

[12] Feng, X.; Gu, J.; Xie, Y.; King, R. B.; Schaefer, H. F. Homoleptic Carbonyls of the Second-Row Transition Metals: Evaluation of Hartree−Fock and Density Functional Theory Methods. *J. Chem. Theory Comput.* **2007,** 3, 1580-1587.

[13] Li, J.; Schreckenbach, G.; Ziegler, T. A Reassessment of the First Metal-Carbonyl Dissociation Energy in $M(CO)_4$ (M = Ni, Pd, Pt), $M(CO)_5$ (M = Fe, Ru, Os), and $M(CO)_6$ (M = Cr, Mo, W) by a Quasirelativistic Density Functional Method. *J. Am. Chem. Soc.* **1995,** 117, 486-494.

[14] Li, J.; Schreckenbach, G.; Ziegler, T. First Bond Dissociation Energy of $M(CO)_6$ (M = Cr, Mo, W) Revisited: The Performance of Density Functional Theory and the Influence of Relativistic Effects. *J. Phys. Chem.* **1994,** 98, 4838-4841.

[15] Li, J.; Schreckenbach, G.; Ziegler, T. Relativistic Effects on Metal-Ligand Bond Strengths in .pi.-Complexes: Quasi-Relativistic Density Functional Study of $M(PH_3)2X2$ (M = Ni, Pd, Pt; $X_2 = O_2$, C_2H_2, C_2H_4) and $M(CO)_4(C_2H_4)$ (M = Fe, Ru, Os). *Inorg. Chem.* **1995,** 34, 3245-3252.

[16] Sharma, S.; Chander, S.; Sehgal, M. L.; Ahmad, I. ^{13}C and ^{17}O NMR of Mono-Nuclear Carbonyls: A DFT Study. *Orient. J. Chem.* **2015,** 31.

[17] Schreckenbach, G.; Ziegler, T. Calculation of NMR Shielding Tensors Using Gauge-Including Atomic Orbitals and Modern Density Functional Theory. *J. Phys. Chem.* **1995,** 99, 606-611.

[18] Schreckenbach, G.; Ziegler, T. Calculation of NMR shielding tensors based on density functional theory and a scalar relativistic Pauli-type Hamiltonian. The application to transition metal complexes. *Int. J. Quant. Chem.* **1997,** 61, 899-918.

[19] Singh, H.; Bhardwaj, A. K.; Sehgal, M. L.; Ahmad, I. Predicting ESR Peaks in Copper (II) Chelates Having Quadrupolar Coordinating Sites by NMR, ESR and NQR Techniques: A DFT Study. *Orient. J. Chem.* **2015,** 31, 671-679.

[20] Singh, H.; Bhardwaj, A. K.; Sehgal, M. L.; Javed, M.; Ahmad, I. Predicting ESR Peaks in Titanium (III), Vanadium (IV) and Copper (II) Complexes of Halo Ligands by NMR, ESR and NQR Techniques: A DFT Study. *Orient. J. Chem.* **2015,** 31, 1461-1468.

[21] Schreckenbach, G. NMR Shielding Calculations across the Periodic Table: Diamagnetic Uranium Compounds. 2. Ligand and Metal NMR. *Inorg. Chem.* **2002,** 41, 6560-6572.

[22] Ruiz-Morales, Y.; Schreckenbach, G.; Ziegler, T. Theoretical Study of 13C and 17O NMR Shielding Tensors in Transition Metal Carbonyls Based on Density Functional Theory and Gauge-Including Atomic Orbitals. *J. Chem. Phys.* **1996,** 100, 3359-3367.

[23] Schreckenbach, G.; Ziegler, T.; Li, J. The implementation of analytical energy gradients based on a quasi-relativistic density functional method: The application to metal carbonyls. *Int. J. Quant. Chem.* **1995,** 56, 477-488.
[24] Autschbach, J. The Calculation of NMR Parameters in Transition Metal complexes. *Structure and Bonding* **2004,** 112, 1-43.
[25] Nakamoto, K. Applications in Inorganic Chemistry. In *Infrared and Raman Spectra of Inorganic and Coordination Compounds*, 4 ed.; John Wiley & Sons, Inc.: 1986; pp 291-298.
[26] Adams, D. M.; Hooper, M. A.; Squire, A. A Raman spectroscopic study of dimanganese and dirhenium decacarbonyls. *J. Chem. Soc. A: Inorg., Phys., Theo.* **1971**, 71-77.
[27] Bor, G. Reassignment of the infrared-inactive C-O stretching frequencies of decacarbonyldimanganese. *J. Chem. Soc. D: Chem. Commun.* **1969**, 641-642.
[28] Flitcroft, N.; Huggins, D. K.; Kaesz, H. D. Infrared Spectra of $(CO)_5Mn\text{-}Re(CO)_5$ and the Carbonyls of Manganese, Technetium, and Rhenium; Assignment of C≡O and M=C Stretching Absorptions. *Inorg. Chem.* **1964,** 3, 1123-1130.
[29] Michels, G. D.; Svec, H. J. Characterization of decacarbonylmanganesetechnetium and decacarbonyltechnetiumrhenium. *Inorg. Chem.* **1981,** 20, 3445-3447.
[30] Vogler, A.; Kunkely, H. Photochemistry of $[MCo_2(CO)_8]$ (M = Zn, Cd, Hg) induced by metal to metal charge tranfer excitation. *J. Organomet. Chem.* **1988,** 355, 1-6.
[31] Baerends, E. J.; Branchadell, V.; Sodupe, M. Atomic reference energies for density functional calculations. *Chem. Phys. Lett.* **1997,** 265, 481-489.
[32] Berry, R. S. Correlation of Rates of Intramolecular Tunneling Processes, with Application to Some Group V Compounds. *J. Chem. Phys.* **1960,** 32, 933-938.
[33] Holmes, R. R. Structure of cyclic pentacoordinated molecules of main group elements. *Acc. Chem. Res.* **1979,** 12, 257-265.
[34] Lauterbur, P. C.; Ramirez, F. Pseudorotation in trigonal-bipyramidal molecules. *J. Am. Chem. Soc.* **1968,** 90, 6722-6726.
[35] Gielen, M. *Advances in Dynamic*
[36] *Stereochemistry*. Freund London: 1995; Vol. 1, p 1-41.
[37] Borisov, Y. A.; Raevskii, N. I. The bond energies in clusters of the elements in the statistical approximation. *J. Struc. Chem.* **1984,** 24, 588-592.
[38] King, R. B. Atomic orbitals, symmetry, and coordination polyhedra. *Coord. Chem. Rev.* **2000,** 197, 141-168.Ryason, P. R. Raman band intensities in binary liquid solutions. *J. Mol. Spec.* **1962,** 8, 164-166.
[39] Schrötter, H. W.; Bernstein, H. J. Intensity in the Raman effect. IX. Absolute intensities for some gases and vapors. *J. Mol. Spec.* **1964,** 12, 1-17.
[40] Tunnicliff, D. D.; Jones, A. C. General basis for quantitative Raman analyses. *Spectrochimica. Acta.* **1962,** 18, 579-584.
[41] Long, D. A.; Gravenor, R. B.; Milner, D. C. Intensities in Raman spectra. Part 8.-Intensity measurements in $CHCl_3$ and $CDCl_3$. *Trans. Farad. Soc.* **1963,** 59, 46-52.
[42] van Gisbergen, S. J. A.; Snijders, J. G.; Baerends, E. J. A density functional theory study of frequency-dependent polarizabilities and Van der Waals dispersion coefficients for polyatomic molecules. *J. Chem. Phys.* **1995,** 103, 9347-9354.
[43] van Gisbergen, S. J. A.; Osinga, V. P.; Gritsenko, O. V.; van Leeuwen, R.; Snijders, J. G.; Baerends, E. J. Improved density functional theory results for frequency-dependent polarizabilities, by the use of an exchange-correlation potential with correct asymptotic behavior. *J. Chem. Phys.* **1996,** 105, 3142-3151.
[44] van Gisbergen, S. J. A.; Snijders, J. G.; Baerends, E. J. Application of time-dependent density functional response theory to Raman scattering. *Chem. Phys. Lett.* **1996,** 259, 599-604.
[45] Osinga, V. P.; van Gisbergen, S. J. A.; Snijders, J. G.; Baerends, E. J. Density functional results for isotropic and anisotropic multipole polarizabilities and C6, C7, and C8 Van der Waals dispersion coefficients for molecules. *J. Chem. Phys.* **1997,** 106, 5091-5101.
[46] van Gisbergen, S. J. A.; Kootstra, F.; Schipper, P. R. T.; Gritsenko, O. V.; Snijders, J. G.; Baerends, E. J. Density-functional-theory response-property calculations with accurate exchange-correlation potentials. *Phys. Rev. A* **1998,** 57, 2556-2571.
[47] Bickelhaupt, F. M.; Baerends, E. J. Kohn-Sham Density Functional Theory: Predicting and Understanding Chemistry. In *Rev. Comput. Chem.*, Lipkowitz, K. B.; Boyd, D. B., Eds. John Wiley & Sons, Inc.: Hoboken, 2007; Vol. 15, pp 1-86.
[48] Cotton, F. A.; Monchamp, R. R. High-resolution infrared spectra and structures of cobalt carbonyls. *J. Chem. Soc.* **1960**, 1882-1885.
[49] Blyholder, G.; Head, J.; Ruette, F. Semi-empirical calculation method for transition metals. *Theoretica. chimica. acta.* **1982,** 60, 429-444.